frontiers in Earth Science

ORIGINAL RESEARCH
published: 04 March 2021
doi: 10.3389/feart.2021.615841

Intensive Wildfire Associated With Volcanism Promoted the Vegetation Changeover in Southwest China During the Permian–Triassic Transition

Yao-feng Cai[1,2], *Hua Zhang*[1]*, *Zhuo Feng*[3] *and Shu-zhong Shen*[4]

[1]State Key Laboratory of Palaeobiology and Stratigraphy, Nanjing Institute of Geology and Palaeontology and Center for Excellence in Life and Paleoenvironment, Chinese Academy of Sciences, Nanjing, China, [2]College of Earth and Planetary Sciences, University of Chinese Academy of Sciences, Beijing, China, [3]Institute of Palaeontology, Yunnan University, Kunming, China, [4]State Key Laboratory for Mineral Deposits Research and School of Earth Sciences and Engineering, Nanjing University, Nanjing, China

OPEN ACCESS

Edited by:
André Jasper, Universidade do Vale do Taquari–Univates, Brazil

Reviewed by:
Dieter Uhl, Senckenberg Research Institute and Natural History Museum Frankfurt, Germany
Jürgen Kriwet, University of Vienna, Austria

***Correspondence:**
Hua Zhang
hzhang@nigpas.ac.cn

Specialty section:
This article was submitted to Paleontology, a section of the journal Frontiers in Earth Science

Received: *10 October 2020*
Accepted: *21 January 2021*
Published: *04 March 2021*

Citation:
Cai Y-F, Zhang H, Feng Z and Shen S-Z (2021) Intensive Wildfire Associated With Volcanism Promoted the Vegetation Changeover in Southwest China During the Permian–Triassic Transition. Front. Earth Sci. 9:615841. doi: 10.3389/feart.2021.615841

Palaeo-wildfire, which had an important impact on the end Permian terrestrial ecosystems, became more intense in the latest Permian globally, evidenced by extensive occurrence of fossil charcoals. In this study, we report abundant charcoals from the upper part of the Xuanwei Formation and the Permian–Triassic transitional Kayitou Formation in the Lengqinggou section, western Guizhou Province, Southwest China. These charcoals are well-preserved with anatomical structures and can be classified into seven distinctive types according to their characteristics. Organic carbon isotopic analyses of both bulk rocks and charcoals show that the $\delta^{13}C_{org}$ values in the Kayitou Formation are notably more negative than those in the Xuanwei Formation, with a negative excursion of 4.08‰ immediately above the volcanic ash bed in the middle of the uppermost coal bed of the Xuanwei Formation. Charcoals with high reflectance values (Ro_{mean} = 2.38%) are discovered below the ash bed. By contrast, the reflectance values (Ro_{mean} = 1.51%) of the charcoals in the Kayitou Formation are much lower than those of the Xuanwei Formation, indicating the palaeo-wildfire types have changed from crown fires to surface fires, which was probably due to the retrogression of vegetation systems during the extinction. Based on the above evidence, we suppose that palaeo-wildfires became more frequent and more severe since the climate became drier during the latest Permian in Southwest China, and the eventual vegetation changeover of the terrestrial ecosystems in Southwest China could be caused by volcanism.

Keywords: charcoal, $\delta^{13}C_{org}$, reflectance, volcanism, late Permian, Southwest China

1 INTRODUCTION

Fire is a considerable disturbance that influences the Earth's ecosystems over both short and long timescales (e. g., Scott, 2000; Sugihara et al., 2006; Belcher et al., 2013). It has been demonstrated that wildfires have played a significant role in many environmental and evolutionary innovations in geological history (Wolbach et al., 1985; Bond and Scott, 2010). Fire activity is suggested to be

very common during the Late Paleozoic according to palaeoatmospheric oxygen estimates (Bergman et al., 2004) and charcoal records from mire settings (Glasspool and Scott, 2010). As the direct evidence of palaeo-wildfire, charcoal particles in the sediments from the Late Paleozoic have been extensively reported all over the world, such as South China (Shen et al., 2011; Zhang et al., 2016; Feng et al., 2020a), North China (Wang and Chen, 2001; Yan et al., 2016; Lu et al., 2020), central Europe (Uhl and Kerp, 2003; Uhl et al., 2008, 2012), Canada (Grasby et al., 2011), Brazil (Manfroi et al., 2015; Kauffmann et al., 2016), India (Jasper et al., 2012; Jasper et al., 2013; Jasper et al., 2016a; Jasper et al., 2016b; Murthy et al., 2020), Australia (Glasspool, 2000; Vajda et al., 2020) and Antarctica (Tewari et al., 2015).

So far, more and more investigations indicate that wildfire, which had an important impact on terrestrial ecosystems, could have contributed to the end-Permian mass extinction (EPME): a change in the maceral composition from Australia indicates that a major fire event resulted in the destruction of vegetation, and increased run-off and erosion on land during the late Permian (Glasspool, 2000); Wang and Chen (2001) proposed that high-frequency wildfires and water-stress might be the main extinction mechanisms for the forest vegetation dieback at the EPME in North China; large-scale combustion of coals and organic-rich sediments induced by the Siberian Traps, was suggested to have affected the global climate change and carbon cycle during the latest Permian (Grasby et al., 2011). The published charcoal records from Permian and Triassic sediments were summarized by Abu Hamad et al. (2012), showing a "charcoal gap" in the Early Triassic.

The records of wildfire are quite abundant in many terrestrial Permian–Triassic (P–T) sequences in China, including the Sandaogou section in Gansu (Wang, 1993), the Dalongkou section in Xinjiang (Cao et al., 2008; Wan et al., 2016; Cai et al., 2019), the Baode section in Shanxi (Wang and Chen, 2001; Lu et al., 2020) and the Guanbachong, Taoshujing, Lubei and several other sections in Southwest China (Shen et al., 2011; Zhang et al., 2016; Yan et al., 2019; Feng et al., 2020a).

The joint area of western Guizhou and northeastern Yunnan provinces in Southwest China has been regarded as an ideal place to investigate the terrestrial EPME because it contains both well-developed marine and terrestrial continuous P–T transitional strata (Wang and Yin, 2001; Peng et al., 2006; Yu et al., 2015; Shen et al., 2011; Zhang et al., 2016). Though the exact P–T boundary in many sections is not precisely defined, the biostratigraphy, chemostratigraphy and geochronology have been investigated for decades in this region. The study of palaeo-wildfires during the P–T transition period in this area has also attracted much attention. Shen et al. (2011) and Zhang et al. (2016) have proposed that the deposition of the Kayitou Formation was dramatically arid, with evidence of abundant fossil charcoals in it. Yan et al. (2019) suggested that the increase of fire activity, evidenced by the increased inertinite in coals, may be a major factor to explain some local oxygen depletion in the marine realm as a result of increase of run-off and erosion after frequent fire activities. Chu et al. (2020) reported an increased abundance of fossil charcoal in the lower part of the Kayitou Formation, which was coincident with the loss of vegetation and the onset of a negative $\delta^{13}C_{org}$ excursion. Among these investigations, little attention has been paid to the anatomical structure and detailed distribution of charcoals along the strata.

In this paper, we systematically analyzed the occurrences, random reflectance values of the charcoals, and the organic carbon isotopes ($\delta^{13}C_{org}$) data of both charcoal and bulk rock samples from the Lengqinggou section in western Guizhou, Southwest China. Our study shed new light on the fire dynamics and vegetation changeover in Southwest China during the P–T transition, and the relationships between palaeo-wildfire, volcanism and carbon cycling.

2 GEOLOGICAL SETTING

In the study area of western Guizhou and eastern Yunnan provinces (WGEY), Southwest China, the Permian–Triassic successive deposits extensively crop out, and have been regarded as a significant window for studying the terrestrial ecosystems at the time (Wang and Yin, 2001; Peng et al., 2006; Shen et al., 2011; Yu et al., 2015; Zhang et al., 2016; Feng et al., 2020b; Liu et al., 2020). During the Permian, this area was situated on the eastern margin of a landmass known as the Khangdian Oldland, which was located near the equatorial zone according to a palaeomagnetic study (Wang and Li, 1998), possessing the distinctive Cathaysian *Gigantopteris* flora of tropical peatlands (Zhao et al., 1980). The strata exposed in this region consist of the middle Permian Emeishan Basalt Formation, the upper Permian Xuanwei Formation, the Permian–Triassic transitional Kayitou Formation and the Lower Triassic Feixianguan Formation (marine)/Dongchuan Formation (terrestrial), in ascending order. Lithofacially, a transgression during the P–T transition is indicated by an upward succession change from terrestrial, to terrestrial–marine transitional, and to marine facies from west to east in WEGY (Yao et al., 1980; Wang, 2011). The Lengqinggou section (104° 20' 13" E; 27° 15' 46" N), is located in Hezhang County of Bijie City, western Guizhou Province (**Figure 1**), and includes terrestrial–marine transitional facies deposits during the Permian–Triassic transition. The strata spanning the P–T boundary in this section include the terrestrial Xuanwei Formation, the terrestrial–marine transitional Kayitou Formation and the marine Feixianguan Formation, in ascending order. The Xuanwei Formation is dominated by yellowish green and greyish green clastic sediments, with intercalations of organic-rich mudstones and coals. Plants of the *Gigantopteris* flora are commonly found in the Xuanwei Formation (Hilton et al., 2004; Yu et al., 2015; Chu et al., 2016; Zhang et al., 2016; Feng et al., 2020b), and include diverse *Lepidodendron*, *Lobatannularia*, *Annularia*, *Calamites*, pecopterids, gigantopterids, cycads and ginkgophytes. The Kayitou Formation mainly comprises mudstones, shales and siltstones, but without coals. Bivalves, gastropods and some plant fragments are commonly observed in the lower part of the formation. This formation is supposed to encompass the terrestrial EPME (Zhang et al., 2016). In this section, the last appearances of *Lepidodendron* and *Gigantopteris* are in the lowermost Kayitou Formation, the roof shale of the

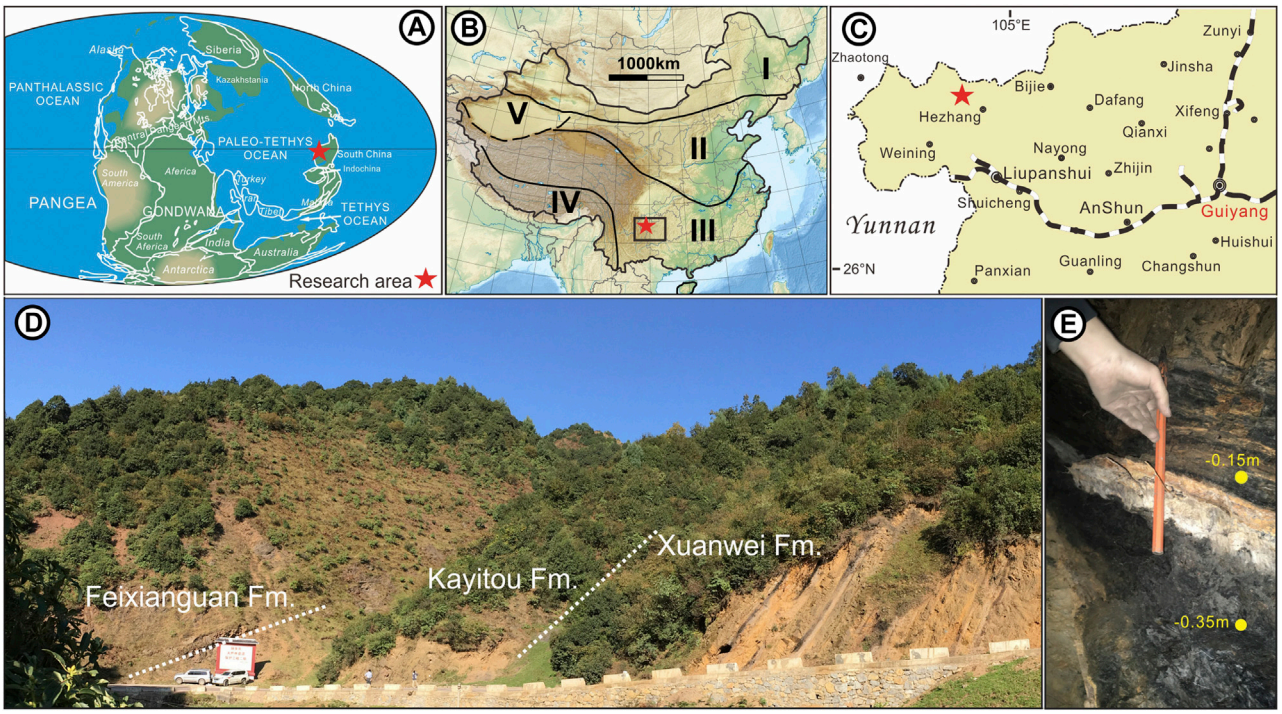

FIGURE 1 | The Lopingian (late Permian) maps, phytogeoprovinces and the location of the studied section. **(A)** Palaeogeographic map of the Lopingian showing the study area (asterisk) (Modified from Scotese, 2001). **(B)** Map showing the location (asterisk) of the study area and late Permian phytogeoprovinces in China (Modified from Shen, 1995). **(C)** Map showing the location of the Lengqinggou section (asterisk). **(D)** Outcrop photo of the Lengqinggou section. **(E)** Photo of the uppermost coal with an ash bed at the top part of the Xuanwei Formation, labeled with sample positions. I- Angara province in Junggar–Hinggan Region; II- Cathaysisa–Euramerica–Angara mixed province; III- Cathaysia province; IV- Gondwana province; V-Angara province in Tarim Plate.

uppermost coal bed of the Xuanwei Formation. Abundant *Tomiostrobus sinensis* were found in a thin bed some 1.2–1.6 m above the uppermost coal bed (Feng et al., 2020b). A mixed marine–non-marine biota appears about 5 m above the uppermost coal bed, and contains fragments of plants, a few brachiopods and bivalves. The Lower Triassic Feixianguan Formation is composed of marine siliciclastic sandstones, mudstones and limestones. It exhibits pure steel gray siltstones in the lower part, and gradually changed to maroon–reddish sandstones and siltstones upward. Fossils are rare in the Feixianguan Formation.

3 MATERIAL AND METHODS

In total, 92 samples (nine from the coal beds and 83 from the clasolite), as fresh as possible, were excavated at the outcrops. The bulk rock samples were crushed into some centimetre-sized pieces, washed with pure water and immersed in hydrochloric acid (10%) for at least 24 h. Then they were neutralized with distilled water, and soaked in hydrofluoric acid for a further week to dissolve the matrix. The remaining matrix was rinsed again, gently washed with distilled water using a 30 μm sieve. After that, the samples were boiled with hydrochloric acid (35%) for 30 min to remove calcium fluoride precipitation, rinsed and dried on a hotplate at about 70°C.

Charcoals showing characteristics such as black colour and streak, silky luster, homogenized cell walls, and well-preserved with anatomical details were picked out from the acid-treated residue under binoculars with the aid of preparation needles, lancets, script liner and tweezers. Selected charcoal samples were investigated using a LEO1530VP scanning electron microscope after gold-coating. All samples were using the same amount throughout the treatment procedure, and charcoals were also calculated quantitatively in detail for statistical analysis.

The charcoal abundance in clastics was quantified by counting the numbers of particles in each single sample, and calibrated to the number per 100 g of sediments. This method was not suitable for coal sample because coal contains large amount of charcoals with much compaction. Instead, the quantification of charcoals in coal samples is represented by a rough percentage of the amount of charcoals in the residues after acid treatment.

Extra residues and some charcoal pieces were analyzed for $\delta^{13}C$ values using a Thermo Fisher Delta V plus + Flash EA HT at the Nanjing Institute of Geology and Palaeontology, Chinese

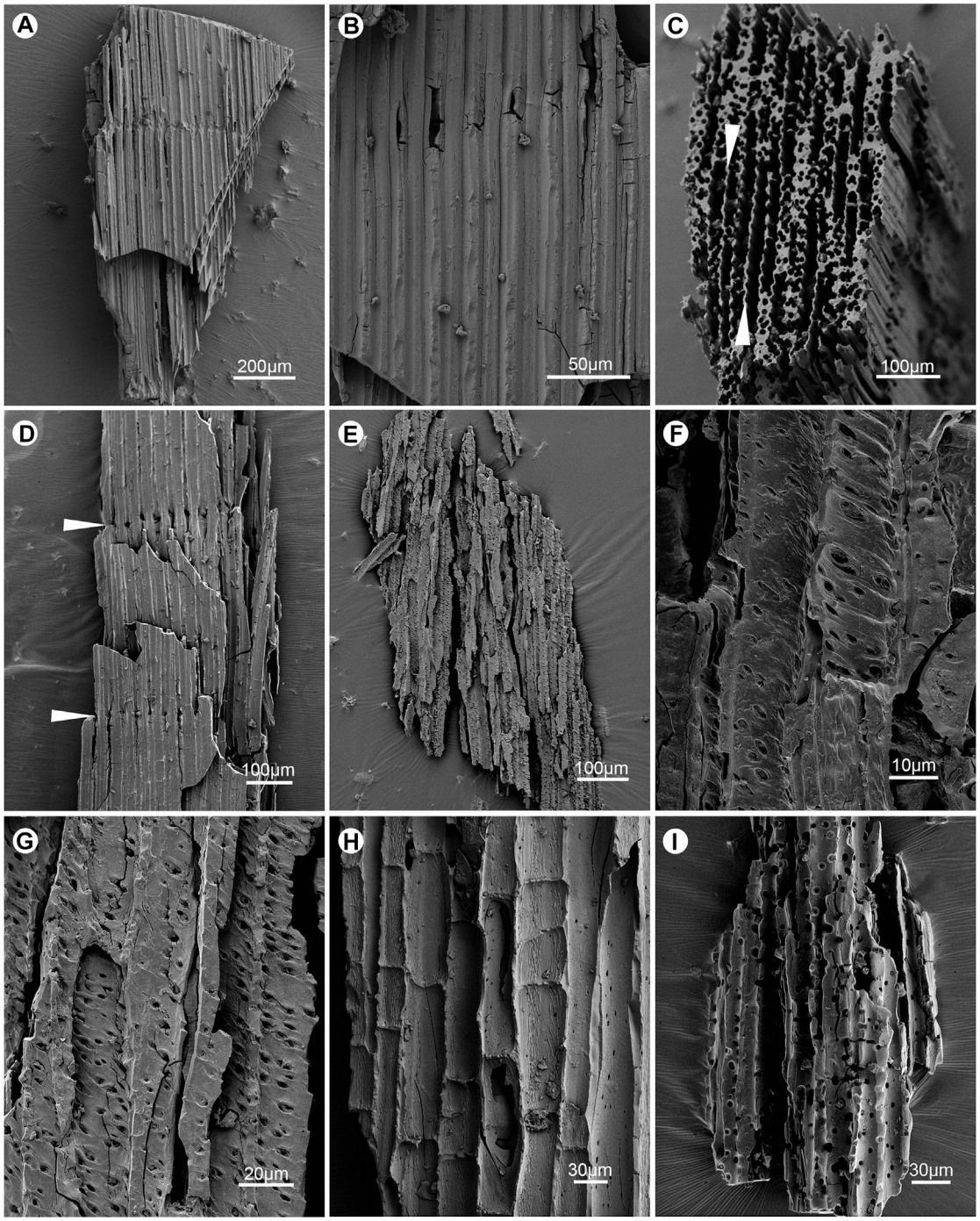

FIGURE 2 | SEM images of charcoal Type 1 **(A–D)** and Type 2 **(E–H)** from the Lengqinggou section in Guizhou Province, Southwest China. **(A)** General appearance of type 1, showing plate-like shape. **(B)** Tracheids show smooth, homogenized walls, without pits. **(C)** Cross section, showing the radial tracheid walls formed straight and continuous lines (arrows). **(D)** Images show radial rows of holes (arrows) on the tracheids. **(E)** Xylem fragment of type 2. **(F–G)** Images showing numerous irregularly distributed pits on the radial tracheid walls. **(H)** Showing axial parenchyma cells. **(I)** Image show charcoal with shot-like holes.

Academy of Sciences. Reproducibility was better than 0.2‰. Organic carbon isotope values are given in per mil (‰) relative to Vienna Peedee Belemnite (VPDB). Reflectance values of charcoals were measured using a Zeiss Axioskop 40 Pol microscope in Nanjing University.

4 RESULTS

4.1 Charcoal Distribution and Preservation

In the Lengqinggou section, there are 50 horizons containing charcoal fragments, with four intervals displaying high

concentration of charcoals. The sample from −25.5 m has the largest amount of charcoals among the clastic samples of the Xuanwei Formation. These charcoals are granulous or blocky, mainly 0.5–1.5 mm in dimension, with limited abraded edges, indicating a low-energy transport. In the interval around −17.8 m, there are three coal beds, in which charcoals are very abundant. The charcoal specimens in this interval are blocky, acicular or flaky, and up to 15 mm in dimension. Another charcoal-rich interval is around −5.7 m, containing several thin coal seams. Charcoals in this interval are mainly blocky and flaky, measuring 1–2 mm in diametre. Considering the non-equidimensional fragmentary nature, sharp edges and the presence of charred cuticles, most of the charcoals in this interval likely experienced a low-energy transport, pointing to parautochthonous deposition. The uppermost charcoal-rich interval is around 8.8 m. The sample residues consist of limited organic matter, but the charcoal particles commonly have well-preserved anatomical structures. They show various sizes, but are generally less than 1.5 mm in dimension, blocky or acicular, representing allochthonous characteristics.

4.2 Description of the Charcoals

Charcoal fragments are very common in the Lengqinggou section, especially in the plant-bearing layers and the coal beds. Although most of the charcoal samples are too small to precisely assess their taxonomy, some charcoals show very distinctive anatomical characteristics, and provide critical information on their affinities. We ascribe the current charcoal samples to seven types based on their gross morphologies and anatomies. These charcoal morphotypes do not necessarily belong to an individual biological species, but may represent different parts/tissues, or the natural variations of various taxa.

Type 1: This type of charcoal is commonly plate-like shaped (**Figure 2A**). The tracheids are long and straight, 10–30 μm wide. Radial tracheid pits are not observed (**Figure 2A,B**). The walls of the tracheids are conspicuously homogenized, 3–5 μm in thickness, and commonly arranged in straight lines forming a flatbed-like structure in cross-section (**Figure 2C**). Sometimes radial rows of holes on tracheids are observed (**Figure 2D**). Rays are not observed.

Type 2: The charcoal particles are irregular shaped and brittle along the tracheids (**Figure 2E**). The tracheids are 20–30 μm wide, exhibiting numerous irregularly distributed pits in the radial walls (**Figure 2F,G**). Pits are 2–3 μm in diametre, and circular or elliptical, with slight borders. Axial parenchyma is sometimes observed (**Figure 2H**).

Remarks: This type is sometimes confused with charcoals that showing shot-like holes in the tracheids cell walls (**Figure 2I**), which produced by fungal hyphae during wood decomposition (El Atfy et al., 2019). However, differences are present. The pits distinguished here are round to elliptical, slightly bordered or embossly lipped (**Figure 2F,G**); while holes produced by brown-rot fungi are all round with sunken edge or not.

Type 3: Charcoals of this type show both primary and secondary xylems (**Figure 3A**). Tracheids of the primary xylem are 15–30 μm wide, with annular and scalariform thickenings (**Figure 3B**). Secondary xylem tracheids are much wider, commonly 60–100 μm wide. Radial tracheid walls show multiseriate (up to 10), alternately arranged, and transversely elongated pits (6–10 μm in diametre) (**Figure 3C,D**). The pits are regularly arranged, showing a mesh-like appearance (**Figure 3C–E**). Araucarioid cross-field pitting is observed, showing three to six pits (3–5 μm in diametre) in each cross-field unit (**Figure 3E**). Uniseriate pits are occasionally observed on the tangential tracheid walls (**Figure 3F**).

Type 4: This type of charcoal is commonly isodiametric or cuboid in shape. Tracheids are 20–30 μm in width, with walls of 3–5 μm thickness (**Figure 3G**). In radial view, they exhibit uniseriate bordered pits on the radial tracheid walls. Pits are commonly in spindle-shapes (5–10 μm in diametre) with oblique apertures, and are discontinuously arranged (**Figure 3H**). The cross-field is araucarioid, showing one to four pits (6–8 μm in diametre) in each cross-field unit (**Figure 3I**).

Type 5: This type commonly is preserved as thin plates (**Figure 4A**). Tracheids are 40–60 μm in width with smooth walls and bent ends. Rays are commonly indicated but usually lost, leaving the cavity in tangential view. The radial tracheid walls exhibit biseriate or triseriate bordered pits (**Figure 4B,C**). The circular pits are about 8 μm in diametre, and alternately, contiguously arranged (**Figure 4C**).

Type 6: The charcoal particles are mainly in regular, quadrilateral tabular or blocky forms. The tracheids are 25–35 μm wide, consisting of 5 μm thick walls (**Figure 4D**). They usually exhibit uniseriate bordered pits, or very rarely biseriate pits on the radial walls. Pits are circular, 12–15 μm in diametre, with circular or elliptical apertures (about 5 μm in diametre), and are mostly separate from each other (**Figure 4E**). The cross-field shows two to four pits (6–8 μm in diametre) with wide, elliptical apertures in each cross-field unit (**Figure 4F**).

Type 7: Charcoals of this type usually exhibit as short columns or strips. The tracheids are approximately 25 μm wide (**Figure 4G**). Bordered pits on the radial tracheid walls are mainly uniseriate, but alternately arranged biseriate pits are very rarely observed. Pits are separated by crassulae (**Figure 4H**). The pits are oval (6–8 μm in diametre) with elliptical apertures. The cross-field is araucarioid, possessing 8–12 pits (4–7 μm in diametre) in each cross-field unit (**Figure 4I**).

4.3 Organic Carbon Isotopes

In the Lengqinggou section, 78 samples (including bulk, coal and charcoal fragments) spanning an 80 m interval from the upper part of the Xuanwei Formation to the upper Kayitou Formation were analyzed. Most of the $\delta^{13}C_{org}$ values in the coal-bearing strata below −0.35 m vary between −23‰ and −24‰, with a mean value of −23.8‰. Samples from −13.69 m and −16.05 m show slightly negative values, −24.18‰ and −24.70‰, respectively. An abrupt negative excursion occurred immediately above the ash bed in the middle of the uppermost coal, with a decrease of 4.08‰. Samples from the overlying Kayitou Formation exhibit $\delta^{13}C_{org}$ values fluctuating around −28‰, with a mean value of −28.2‰, which notably differs from the mean value (−23.8‰) in the Xuanwei Formation. A negative spike with the $\delta^{13}C_{org}$ value of −30.24‰ appears at

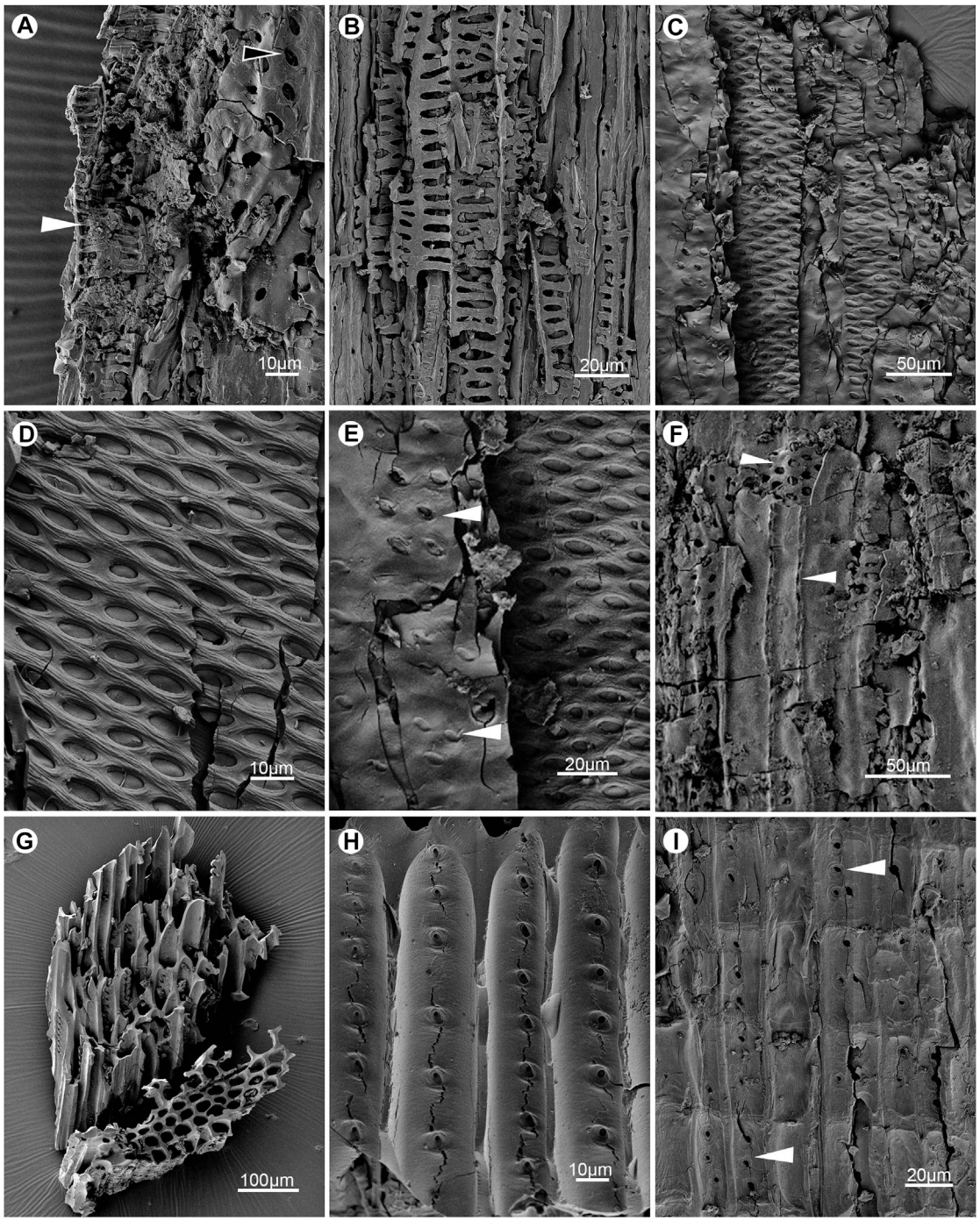

FIGURE 3 | SEM images of charcoal Type 3 **(A–F)** and Type 4 **(G–I)** from the Lengqinggou section in Guizhou Province, Southwest China. **(A)** Primary xylem tracheid with annular wall thickenings (white arrow) and secondary xylem tracheid with multiseriate pits (black arrow). **(B)** Primary xylem tracheids exhibit scalariform thickenings. **(C)** Image of secondary xylem tracheids, showing multiseriate pits on the radial walls. **(D)** Secondary xylem tracheid shows multiseriate, alternately arranged, and transversely elongated radial pits. **(E)** Higher magnification image of Fig. C, showing 36 pits in cross-fields (arrows). **(F)** Tangential view of tracheids, showing distinct pit cavities (lower arrow), bend radial wall with bordered pit (upper arrow) and smooth tangential wall. **(G)** Charcoal of type 4. **(H)** Radial view, showing uniseriate, discontiguous pits on the radial tracheid walls. **(I)** Cross-fields with 1–4 pits (arrows).

10.7 m. The anomalous isotopic interval continued throughout the remaining parts of the Kayitou Formation, and gradually recovered to the value of about −25‰.

The $\delta^{13}C_{org}$ data of charcoal fragments show that 62.5% values are more positive than those of the bulk rock or coal samples from the same horizon, whereas 37.5% values are

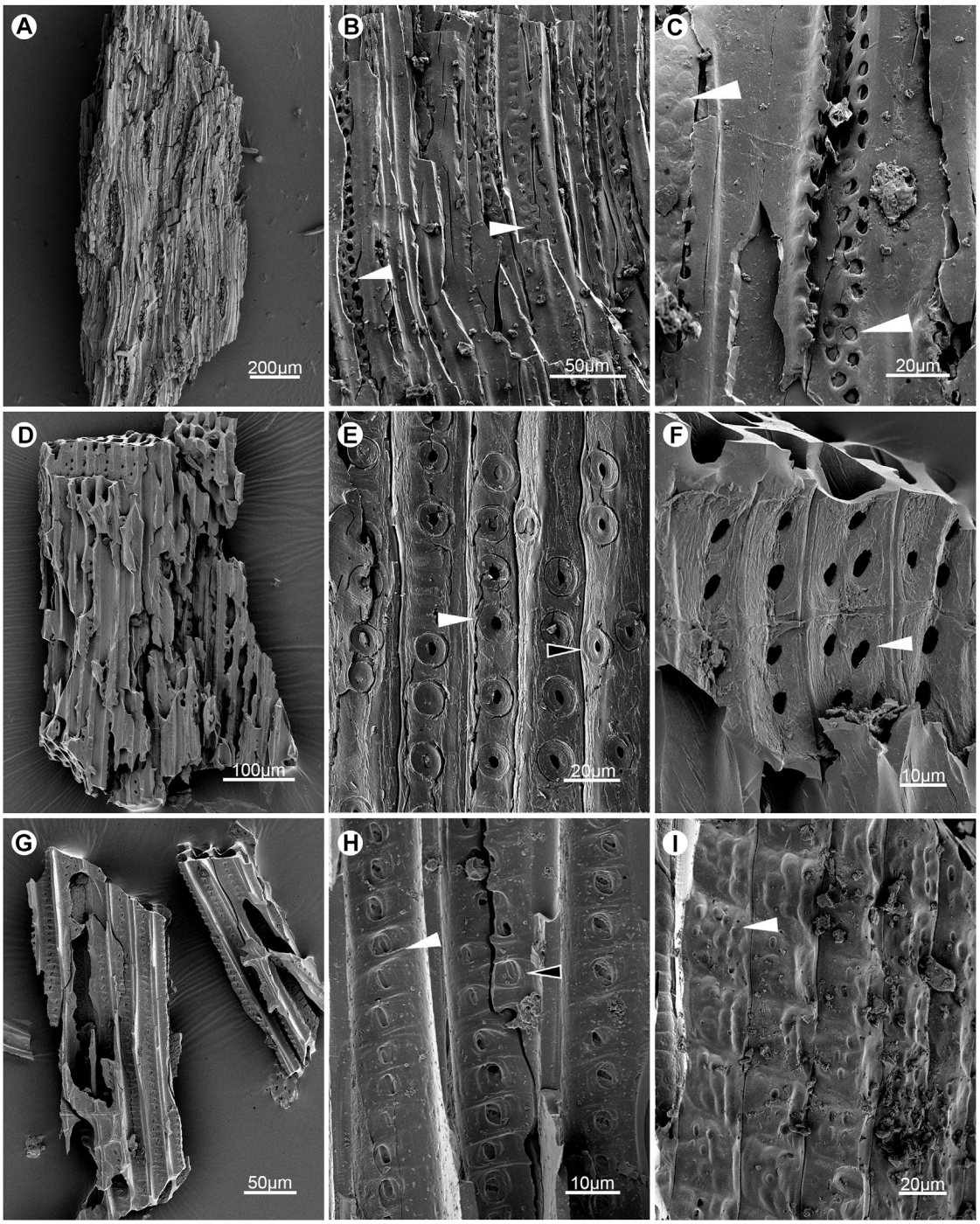

FIGURE 4 | SEM images of charcoal Type 5 **(A–C)**, Type 6 **(D–F)** and Type 7 **(G–I)** from the Lengqinggou section in Guizhou Province, Southwest China. **(A)** Tangential view, showing the common occurrences of rays. **(B)** Oblique radial view of tracheids, showing uni- and biseriate bordered pits on the radial walls (arrows). **(C)** Detail image of radial walls, exhibiting biseriate, alternate pits. **(D)** Xylem fragment of Type 6. **(E)** Radial view of tracheids, showing mainly uniseriate, discontiguous bordered pits (arrows). **(F)** Cross-fields, showing 2–4 pits per field. **(G)** Xylem fragment of Type 7. **(H)** Radial view of tracheids, showing uniseriate, discontiguous pits that separated by crassulae (white arrow); and occasional occurrence of alternately arranged biseriate pits (back arrow). **(I)** Cross-fields, showing numerous pits in each cross-field unit.

more negative. In general, the $\delta^{13}C_{org}$ values between charcoal and bulk samples show a difference from 0.13 to 2.72‰. Only one charcoal exhibits a larger excursion of 9.15‰ in $\delta^{13}C_{org}$ value than that of the coal sample from the same horizon. Detailed organic carbon isotopic data are shown in **Table 1** and **Figure 5**.

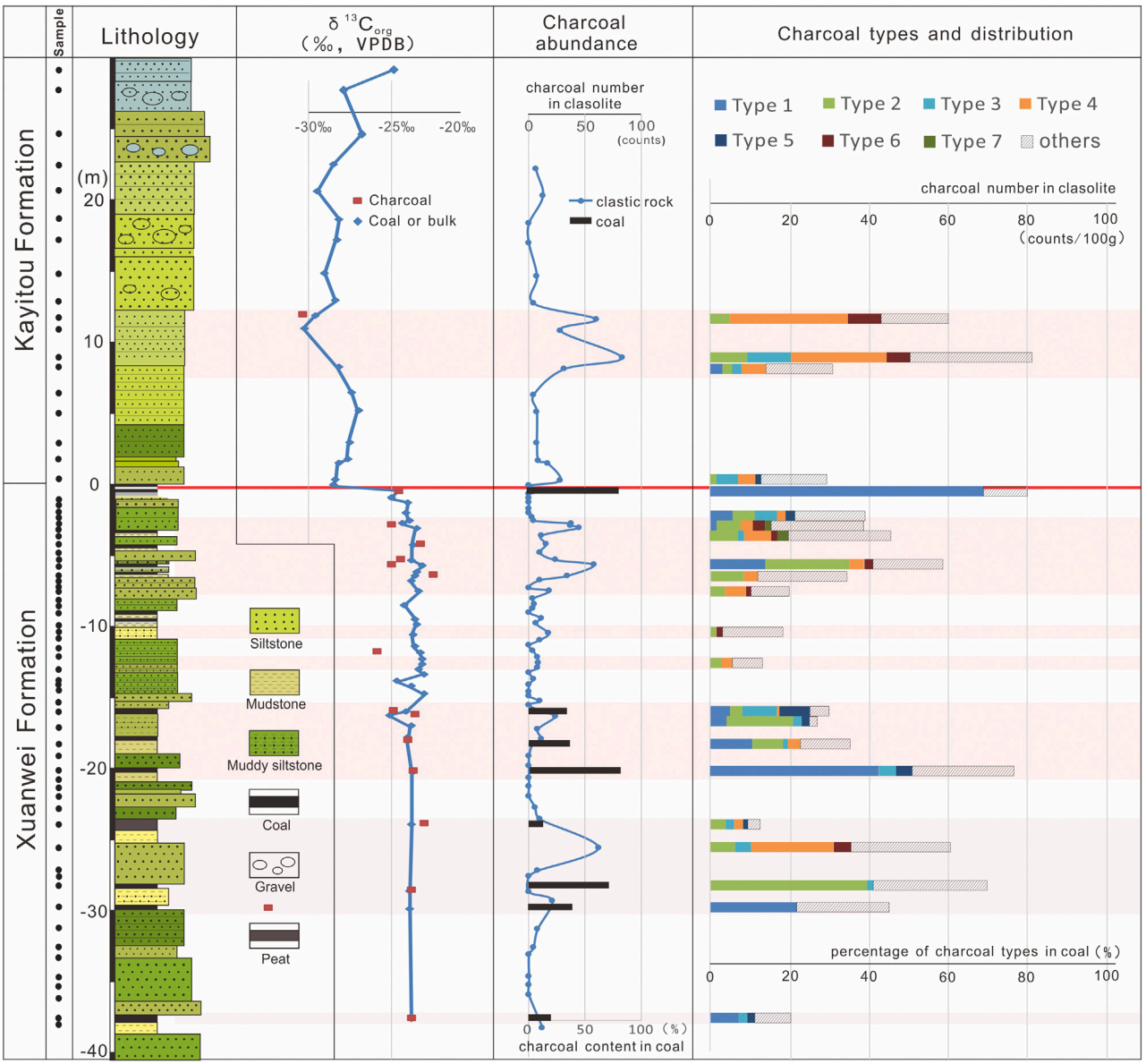

FIGURE 5 | Stratigraphic column and the organic carbon isotopes ($\delta^{13}C_{org}$), charcoal abundance and types of fossil charcoals in the Lengqinggou section, Guizhou Province, Southwest China. The diagram shows sediment logs and thickness in meters. $\delta^{13}C_{org}$ of charcoals are represented by red squares, whereas $\delta^{13}C_{org}$ of coals or bulk rocks are represented by blue rhombuses. The red line represents the position of ash bed in the last coal. Charcoal abundance is counted by numbers in per 100 g samples (clastic rocks) and percentage in residues after acid treatment (coals).

4.4 Charcoal Reflectance

Fifteen pieces of charcoals from two horizons, at −0.35 and 8.8 m, were measured for random reflectance, and results are listed in **Table 2**. Among the charcoals from −0.35 m, Ro values varied from 1.625 to 3.579%, mostly being larger than 2%, with the Ro_{mean} = 2.379%. By contrast, the samples from 8.8 m show much lower random reflectance values, mainly fluctuating around 1.0–1.6%, with a mean value of 1.509%. Only two pieces of charcoal show higher Ro values that are larger than 2%, and the largest Ro value is 2.67%.

5 DISCUSSION

5.1 Taphonomy of the Charcoals

Geochemical and mineralogical studies have indicated a stable sediment source between the upper Permian and the lower Triassic formations in SW China (He et al., 2007; Zhou et al., 2014). At outcrop section, the Xuanwei Formation and the Kayitou Formation exhibit similar lithologic character except for the presence of coals (Bureau of Geology and Mineral Resources of Guizhou Province, 1987). The clastic rocks of the two formations

TABLE 1 | $\delta^{13}C_{org}$ data of bulk rocks, coals and charcoals from the Lengqinggou section in Guizhou Province, Southwest China.

Sample (m)	$\delta^{13}C_{org}$ (‰)	Sample (m)	$\delta^{13}C_{org}$ (‰)	Sample (m)	$\delta^{13}C_{org}$ (‰)	Sample (m)	$\delta^{13}C_{org}$ (‰)
41.5	−25.471	0.2	−28.177	−6.77	−23.32	−16.81	−23.298
33.1	−26.503	−0.15 (coal)	−28.344	−7.53	−22.814	−17.8 (coal)	−23.497
29	−24.598	−0.35 (coal)	−24.26	−8.44	−23.743	−17.8 (charcoal)	−23.43
27.67	−27.973	−0.35 (charcoal)	−24.01	−9.43	−23.041	−17.57	−23.579
24.68	−26.863	−1.06	−24.588	−9.81	−22.946	−20 (coal)	−23.219
22.02	−28.291	−1.34	−23.501	−10.49	−23.188	−20 (charcoal)	−23.037
20.13	−29.355	−2.09	−23.627	−11.33	−23.055	−23.6 (coal)	−23.232
18.19	−27.987	−2.62	−23.451	−11.71	−22.733	−23.6 (charcoal)	−22.375
16.8	−28.111	−2.81	−23.848	−11.7 (charcoal)	−25.451	−28.2 (coal)	−23.365
14.5	−28.926	−2.95 (charcoal)	−24.481	−12.17	−22.535	−28.2 (charcoal)	−23.166
12.6	−28.171	−3.12	−22.956	−12.55	−22.608	−29.4 (coal)	−23.349
11.5	−29.568	−4.26	−23.185	−12.93	−22.795	−29.4 (charcoal)	−32.498
11.5 (charcoal)	−30.237	−4.26 (charcoal)	−22.605	−13.23	−22.499	−36.4 (coal)	−23.257
10.7	−30.237	−5.36	−23.264	−13.69	−24.182	−36.4 (charcoal)	−23.124
8	−28.041	−5.36 (charcoal)	−23.92	−14.07	−23.306	−56.8	−22.526
6.2	−27.143	−5.7	−22.556	−14.6	−22.432	−60.4	−22.503
5	−26.709	−5.7 (charcoal)	−24.464	−15.8 (coal)	−23.596	−66 (coal)	−23.429
2.8	−27.341	−6.2	−22.949	−15.8 (charcoal)	−24.393	−66 (charcoal)	−22.406
1.6	−27.448	−6.46	−23.083	−16.05	−24.701		
1.4	−28.031	−6.46 (charcoal)	−21.792	−16.05 (charcoal)	−22.881		

TABLE 2 | Reflectance data of the charcoals from the horizons of −0.35 m and 8.8 m of the Lengqinggou section in Guizhou Province, Southwest China.

Horizons(m)	Random reflectance (%)								Ro_{mean}	Ro_{max}
−0.35	2.394	2.278	2.429	1.913	1.625	2.431	3.579		2.379	3.579
8.8	1.044	1.297	1.020	1.560	2.670	2.110	1.128	1.242	1.509	2.670

are about the same mineral composition and granularity, indicating a similar sedimentary environment and stable accumulation rate. Thus, all the charcoals from the same host sediments experienced similar compaction and fragmentation during transport and deposit, with limited taphonomic biases.

Experimental analyses have been carried on to assess the impact of post-depositional processes on charcoal preservation (Lancelotti et al., 2010; Chrzazvez et al., 2014), which shows that charcoals are resistant to pressure (up to 22.5 MPa), dimension and number of small fragments are mainly dependent on the charring temperature and the species. Therefore, the charcoal abundance of certain size and variation of different types in a certain depositional condition of the host sediments can be indicators of fire activity and vegetation (Mahesh et al., 2015).

In natural wildfires, microscopic charcoal (<180 μm) can float and transport by wind in long distance (Clark and Patterson, 1997), while mesoscopic (180 μm–1 mm) and macroscopic (>1 mm) charcoals are usually carried by water and deposit near the area of wildfire (Peters and Higuera, 2007; Favilli et al., 2010). Charcoal assemblages comprising variable size and organs may imply minimal transport and local fires (Scott, 2010). Materials in this study are mainly mesoscopic and macroscopic charcoals, and that from Xuanwei Formation are commonly accompanied by other charred plant remains like leaf fragment, megaspore and twig (**Figure 6**), indicating autochthonous or parautochthonous depositions. For morphology, charcoals from clastic rocks in the Xuanwei Formation, as mentioned in results, are mostly granulous or blocky with slightly sorted dimension and limited abraded edges, indicating a parautochthonous deposition; that from coal beds are blocky, acicular or flaky with varied size (up to 15 mm), implying autochthonous deposition. Charcoals from the Kayitou Formation mainly exhibit less variable size with minimized abrasion, also implying allochthonous deposition after short transport by fluvial processes (Nichols et al., 2000).

There is a remarkable taphonomic phenomenon that sample −0.35 m exhibited the greatest charcoal concentration, while sample −0.15 m above an ash contained few charcoals. The macroscopic charcoal assemblage showed varied size and no abrasion, indicating an autochthonous deposition with minimal transport rather than taphonomic bias. Similar pattern represented by the highest reflecting inertinite right under a tonstein layer have been reported nearby (Yan et al., 2019). Volcanism is one of the most common reasons that trigger wildfires in geological history (Scott, 2000), which lead to charcoal accumulation along with pyroclastics. A volcanic-derived cause is speculated here based on the distribution of charcoals and ash in the last coal.

5.2 Wildfire Implications

Fossil charcoals in sediments, as well as inertinite in coal beds, are widely accepted as a key index of palaeo-wildfires in deep time (Scott, 1989, Scott, 2000; Scott and Glasspool, 2007). Wang (2015) and Yan et al. (2019) have reported that the inertinite

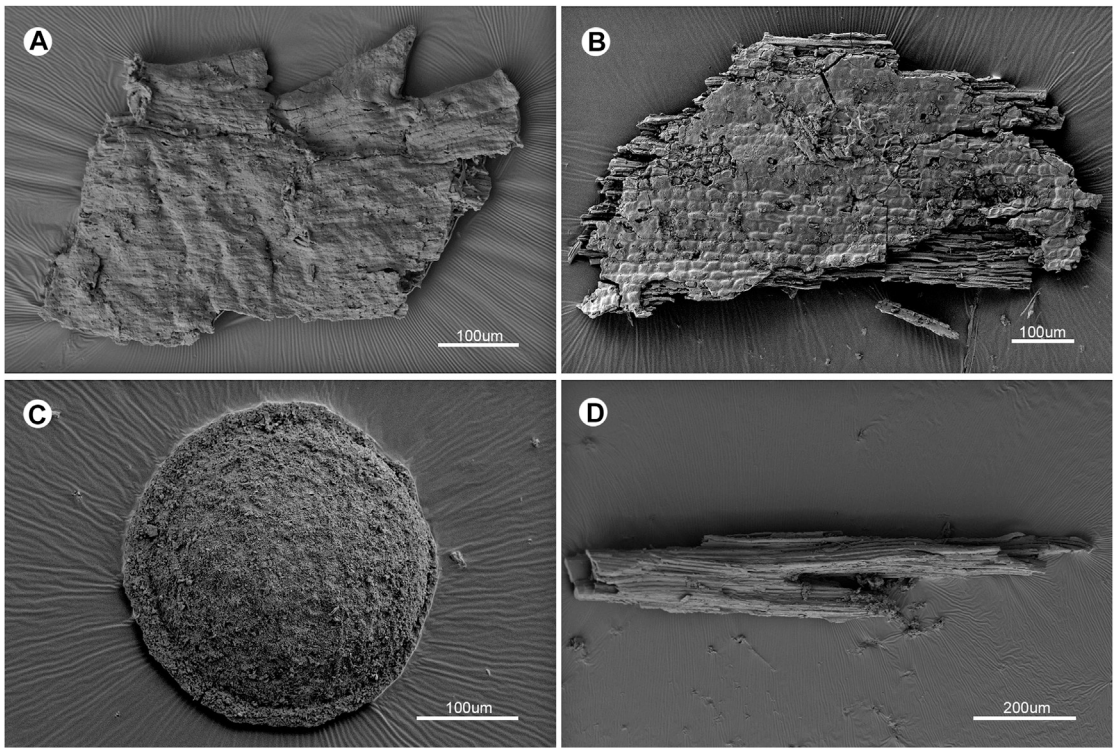

FIGURE 6 | SEM images of charred plant remains from clastic rocks of the Xuanwei Formation. **(A)** Charred leaf fragment shows serrated edge. **(B)** Charred epidermis of plants with molten cuticle and vascular tissue. **(C)** Accompanying megaspore acquired from clastic rocks of the Xuanwei Formation. **(D)** Charred twig with a branch.

content in the coals from the Xuanwei Formation display a steady increase in ascending stratigraphic sequence. Abundant charcoal materials have been previously recognized in the Kayitou Formation at Guanbachong, Longmendong, Lubei and several other sections in Southwest China (Shen et al., 2011; Zhang et al., 2016; Feng et al., 2020a). In this study, we report more than 50 horizons in the Lengqinggou section containing charcoal fragments from the upper Xuanwei and the Kayitou formations, indicating that palaeo-wildfires are common and frequent phenomena during the latest Permian in Southwest China.

Wildfire dynamics during the P–T transition in the Lengqinggou section are represented by the change of charcoal abundance (**Figure 5**). Below the horizon of −15 m, charcoals are mainly collected from coals, except for the specimen from −25.5 m. The samples from coal seams contain a high content of charcoal, mostly higher than 30%, suggesting that wildfires commonly occur in the ever-wet tropical peatland vegetation system. These high contents of charcoal are consistent with the previously documented inertinite content data from the coals in the upper Xuanwei Formation (Yan et al., 2019) and other comparable Changhsingian-aged coals (Glasspool and Scott, 2010). Samples from −20 and −28.2 m show notable charcoal content of about 75%, indicating more frequent and intense wildfires during the peat-forming period. In general, charcoal tends to be more abundantly concentrated in coals compared with the rapid deposits of clastic sediments. The occurrence of abundant charcoal recovered from the clastic rock sample at the horizon of −25.5 m is more likely to indicate an intense fire activity. In the interval between −15 and −2.36 m, charcoals in the clastic rocks are increasing in abundance, from about 10 to 20 particles in each 100 g samples to a peak of about 50 particles per sample. Coals, however, become thinner upward in this interval. It is probably because the climate began drying out during this time, and the aridic tendency led to frequent and widespread, intense wildfires.

The uppermost coal bed at the Lengqinggou section comprises a thick volcanic ash layer in the middle of the coal (**Figure 1E**). Two coal samples below and above the ash layer have been analyzed for charcoal contents, but show completely adverse results. The sample (−0.35 m) below the ash shows the highest charcoal content among the coal samples. By contrast, the sample (−0.15 m) above the ash contains very few charcoals. We speculate that volcanism is the main dynamic causing extensive wildfires and leading to the retrogression of vegetation, so that charcoals were abundantly formed below the ash layer, but very rare above the ash layer.

Above the uppermost coal bed, charcoals are rarely observed until about 8 m. This phenomenon suggests that wildfires were rare during this period, or fuels were rare at the time. Another charcoal abundance peak appeared in the interval from 8 to 11.5 m, which indicates that wildfires reemerged in the terrestrial ecosystems, with sufficient fuel.

5.3 The Turnover of Vegetation

Combined with previous researches about plant succession (Peng et al., 2006; Feng et al., 2020b), the distribution and abundance changes of charcoal types are most likely to support a vegetation turnover from the upper Xuanwei Formation to the lower Kayitou Formation (**Figure 5**). Charcoal types 1, 2 and 3 are mainly distributed in coals of the Xuanwei Formation. In the clastic rocks of the Xuanwei Formation they also account for more than 50% of the total charcoals, but in the Kayitou Formation they became very few. Types 4 and 6 exhibit an opposite characteristic, occupying only a small proportion in the samples from the Xuanwei Formation, but increased substantially in the samples from the Kayitou Formation. Types 5 and 7 are only observed in the Xuanwei Formation.

The reflectance values of the charcoals also indicated a retrogression of the plant community, as the Ro values remarkably declined from the top of the Xuanwei Formation to the lower–middle Kayitou Formation. It has been demonstrated that charcoal reflectance increases with charring temperature (Scott and Glasspool, 2007; McParland et al., 2009; Scott, 2010). Thus, the Ro_{mean} (2.379%) and Ro_{max} (3.579%) from −0.35 m represent a much higher fire temperature formed during crown fires. On the contrary, Ro_{mean} (1.509%) and Ro_{max} (2.670%) from 8.8 m indicate the charcoals were formed at a lower fire temperature during brief surface fires. This phenomenon is consistent with the turnover of vegetation from rainforest to herblands in the lower Kayitou Formation (Feng et al., 2020a, b).

A similar pattern of biological evolution has been reported in several sections in WEGY (Zhang et al., 2016). The highly diversified *Gigantopteris* flora disappears in the lower parts of the Kayitou Formation, followed by the occurrence of a few opportunistic plant elements, a conchostracan fauna and mixed terrestrial–marine biota (Chu et al., 2016; Scholze et al., 2020). In the coal sample (−0.35 m) below the ash bed, charcoals are extremely abundant, with a large proportion of charcoal Type 1, which is different from other coal samples that contain diverse charcoal types. In general, sediment accumulation in peats is much slower than in fluvial environments. Thus, the charcoals deposited in coals could come from different habitats like highland or shoreside and show a high diversity of the plant resource. However, the coal sample from −0.35 m consists almost entirely of charcoal Type 1. One possibility could be that the plant community in the peat represents a monospecific vegetation, but abundant megafossil plant specimens, including *Lepidodendron* and gigantopterids in the roofshale of the coal bed, do not support this assumption. Another possibility could be that the charcoals were formed and accumulated in a very short time, representing the predominant plant species that produced charcoal Type 1.

In addition to the occurrences of extensive wildfires, prevalent drought climate conditions (Shen et al., 2011; Zhang et al., 2016) and a series of volcanisms (Fang et al., 2017; Xu et al., 2017; Hong et al., 2019) were previously documented in Southwest China during the latest Permian. Therefore, the rainforest ecosystems formed by the *Gigantopteris* flora could be severely affected. We speculate that an extreme large volcanic eruption, which formed the thick ash bed, induced extensive wildfires, and destroyed the plant community and buried plenty of charcoal. The *Gigantopteris* flora suffered a devastating strike and disappeared after this event, leaving the last appearance of its fossil record in the lowermost part of the Kayitou Formation. Shortly afterward, opportunistic elements, including the lycopod *Tomiostrobus sinensis* and seed-fern *Germaropteris martinsii*, occupied the niche quickly and formed unique monospecific vegetation in the shoreline environments and the upland environments, respectively (Feng et al., 2020a; Feng et al., 2020b).

5.4 $\delta^{13}C_{org}$ Excursion and Volcanism

Previous studies indicated that carbon isotopes from both marine and terrestrial sections exhibit significant and fast negative excursions around the P–T boundary (Cao et al., 2002, 2008; Xie et al., 2007; Shen et al., 2011, 2013; Zhang et al., 2016; Cui et al., 2017). However, the trigger of this global excursion is still under debate, though several mechanisms have been proposed up to now, such as Siberian Traps volcanism (Korte et al., 2010; Burgess and Bowring, 2015; Cui and Kump, 2015), methane eruptions from thermal destabilization of high-latitude clathrate deposits (Krull et al., 2004; Retallack and Jahren, 2008), the oxidation of organic matter caused by a massive regression (Heydari et al., 2003) and combinations of multiple processes (Zhong et al., 2018).

Organic carbon isotopes of the terrestrial P–T sections in WEGY have been intensively investigated in recent years. Zhang et al. (2016) reported $\delta^{13}C_{org}$ from four terrestrial sections in Southwest China, revealing that the coal-bearing Xuanwei Formation and the lower part of the Kayitou Formation have generally stable organic isotope values about −24.12‰, while a 5–8‰ depletion occurred in the middle part of the Kayitou Formation. Cui et al. (2017) also analyzed $\delta^{13}C_{org}$ from four sections representing terrestrial to marine transitional settings, characterizing a negative shift of 2–3‰ at the top of the Xuanwei Formation. In the Lengqinggou section, the stable organic carbon isotope values do not extend to the Kayitou Formation, the rapid negative excursion begins at the uppermost coal bed and reached a maximal $\delta^{13}C_{org}$ value of −30.237‰ in the lower part of the Kayitou Formation.

Many factors could influence the $\delta^{13}C_{org}$ value in terrestrial environments because of the diverse contributing sources and fractionation (Tieszen and Boutton, 1989), such as variations of plant type (Diefendorf et al., 2010), climate change (Wang et al., 2003), methanotrophic activity (Krull and Retallack, 2000) and other environmental factors affecting the photosynthetic pathways, like atmospheric CO_2 concentration (Schubert and Jahren, 2012), and $\delta^{13}C$ value of the atmosphere (Arens et al., 2000).

In our study, the 4.08‰ negative carbon isotope excursion (NCIE) is not likely caused by long-term processes, such as climate change, vegetational changeover and alternation of sedimentary facies. By contrast, some transient incidents, such as rapid change of atmospheric $\delta^{13}C$ and atmospheric pCO_2 level, and/or massive oxidation of ^{12}C enriched organic material, are more likely the causal mechanism. Recent investigations suggested that volcanism is an adequate explanation for the short-term geochemical changes that caused the negative excursion of $\delta^{13}C_{org}$, as well as other short-lived events like a breakdown of the terrestrial ecosystem could control the rapid latest Permian NCIE (Korte et al., 2010; Chu et al., 2016; Dal Corso et al., 2020). Our data indicate that volcanism was likely the primary cause of the sudden NCIE in the Lengqinggou section, for a 4.08‰ negative excursion occurred just below (−24.26‰) and above (−28.34‰) the ash bed in the last coal. Extensive volcanism was

coincident with the EPME (Erwin, 1994; Jin et al., 2000), and the PTB sequences in southwestern China contain numerous ash beds (Fang et al., 2017; Xu et al., 2017; Hong et al., 2019). According to trace elements and Hf-isotope analyses, these ash beds were mainly deposited locally around the Tethys region (Wang et al., 2019). The volcanism derived from a continental volcanic arc could release a massive amount of CO_2 and lead to rapid changes of atmospheric pCO_2 level and $\delta^{13}C$. The magma or falling spark would induce widespread wildfires on land, and ^{13}C-depleted CO_2 can be generated by interactions between volcanic material and organic-rich sediments (Svensen et al., 2009; Korte et al., 2010; Grasby et al., 2011; Black et al., 2012). The perturbations in atmospheric and carbon-cycle systems would then result in the negative shift of $\delta^{13}C$ values. In the Lengqinggou section, the abrupt negative excursion of $\delta^{13}C_{org}$ above the ash bed and the high concentration of charcoals below the ash bed reinforce our explanation. The massive release of ^{13}C-depleted volcanogenic carbon and associated oxidation of organic matter are therefore suspected to be the direct causes of the negative shift of $\delta^{13}C_{org}$ in this region.

The fluctuations of $\delta^{13}C_{org}$ values in the Kayitou Formation are probably not restricted to the influence of marine organic matter, but also to the influence of terrigenous materials like charcoal. This is evidenced by the apparent correlation between the charcoal abundance and the $\delta^{13}C_{org}$ data in the Kayitou Formation (**Figure 5**). $\delta^{13}C_{org}$ analysis of single charcoal particles showed that most of the charcoal fragments have more positive $\delta^{13}C_{org}$ values, though varying a little in amplitude. $\delta^{13}C_{org}$ values of charcoal are influenced by many factors like material and combustion temperature (Turekian et al., 1998; Poole et al., 2002, Poole et al., 2004; Turney et al., 2006; Hall et al., 2008). Charcoals are derived from plants, as a significant component of organic carbon burial, so their carbon isotope values should mainly respond to the change of atmospheric composition. We believe that the massive volcanic activities and turnover of vegetation altered the atmospheric pCO_2 level and $\delta^{13}C$, which significantly impacted $\delta^{13}C$ of plants, and resulted in ^{12}C-enriched organic carbon burial and then contributed to marine ecosystems through erosion and runoff.

6 CONCLUSION

Charcoals obtained from the upper part of Xuanwei and the Kayitou formations in the Lengqinggou section indicate that wildfire was a prevalent phenomenon during the late Permian, and became more frequent and intensified at the end of the Permian. According to the morphological and anatomical characteristics, the charcoals from the Lengqinggou section were divided into seven types. The abundance of different charcoal types supported the turnover of vegetation type occurring in the lower part of the Kayitou Formation, which is also supported by the charcoal reflectance analysis. $\delta^{13}C_{org}$ analysis of bulk rock, coal and charcoal samples exhibits a sudden 4.08‰ negative excursion at the top of the Xuanwei Formation, and a general 4–6‰ negative excursion in the lower part of the Kayitou Formation. The 4.08‰ negative excursion occurred across the ash bed in the middle of the uppermost coal of the Xuanwei Formation and demonstrates that an intense volcanic activity could be the primary cause for the negative $\delta^{13}C_{org}$. The devastating wildfires that occurred in the latest Permian, evidenced by the extreme charcoal enrichment below the ash bed, promoted the turnover of vegetation. The massive releases of ^{13}C-depleted CO_2 from massive volcanic activities, quick oxidation of organic matter and other associated reactions could lead to rapid changes of atmospheric pCO_2 level and $\delta^{13}C$ values, and caused the negative $\delta^{13}C_{org}$ excursion in the Kayitou Formation.

DATA AVAILABILITY STATEMENT

The original contributions presented in the study are included in the article/Supplementary Material, further inquiries can be directed to the corresponding author.

AUTHOR CONTRIBUTIONS

HZ designed the research and led a team to collect the samples in the field. YFC completed most of the analyses. YFC, ZH and ZF wrote the paper with inputs from SZS. All the authors joined in the revisions, discussions and improvements of the manuscript.

FUNDING

This work was supported by the Strategic Priority Research Programs (B) of the Chinese Academy of Sciences (XDB26000000, XDB18000000) and the National Natural Science Foundation of China (Grant Nos. U1702242, 41502023) and CAS (QYZDY-SSW-DQC023).

ACKNOWLEDGMENTS

We thank two reviewers and the editor for their very useful comments and suggestions to improve the manuscript.

REFERENCES

Abu Hamad, A. M. B., Jasper, A., and Uhl, D. (2012). The record of Triassic charcoal and other evidence for palaeo-wildfires: signal for atmospheric oxygen levels, taphonomic biases or lack of fuel? *Int. J. Coal Geol.* 96, 60–71. doi:10.1016/j.coal.2012.03.006

Arens, N., Jahren, A., and Amundson, R. (2000). Can C_3 plants faithfully record the carbon isotopic composition of atmospheric carbon dioxide? *Paleobiology* 26, 137. doi:10.1666/0094-8373(2000)026<0137:CCPFRT>2.0.CO;2

Belcher, C. M., Collinson, M. E., and Scott, A. C. (2013). "A 450-million-year history of fire," in *Fire phenomena and the earth system (an interdisciplinary Guide to fire science.* Oxford: John Wiley and Sons, 229–249.

Bergman, N. M., Lenton, T. M., and Watson, A. J. (2004). COPSE: a new model of biogeochemical cycling over Phanerozoic time. *Am. J. Sci.* 304, 397–437. doi:10.2475/ajs.304.5.397

Black, B. A., Elkins-Tanton, L. T., Rowe, M. C., and Peate, I. U. (2012). Magnitude and consequences of volatile release from the Siberian Traps. *Earth Planet. Sci. Lett.* 317, 363–373. doi:10.1016/j.epsl.2011.12.001

Bond, W. J., and Scott, A. C. (2010). Fire and the spread of angiosperms in the Cretaceous. *New Phytol.* 118, 1137–1150. doi:10.1111/j.1469-8137.2010.03418.x

Bureau of Geology and Mineral Resources of Guizhou Province (1987). *Regional Geology of Guizhou province*. Beijing,China: Geological Publishing House, 698.

Burgess, S. D., and Bowring, S. A. (2015). High-precision geochronology confirms voluminous magmatism before, during, and after Earth's most severe extinction. *Sci. Adv.* 1 (7), e1500470. doi:10.1126/sciadv.1500470

Cai, Y. F., Zhang, H., Feng, Z., Cao, C. Q., and Zheng, Q. F. (2019). A *Germaropteris*-dominated flora from the upper Permian of the Dalongkou section, Xinjiang, Northwest China, and its paleoclimatic and paleoenvironmental implications. *Rev. Palaeobot. Palynol.* 266, 61–71. doi:10.1016/j.revpalbo.2019.01.006

Cao, C. Q., Wang, W., and Jin, Y. G. (2002). Carbon isotope excursions across the Permian–Triassic boundary in the Meishan section, Zhejiang Province, China. *Chin. Sci. Bull.* 47, 1125–1129. doi:10.1360/02tb9252

Cao, C. Q., Wang, W., Liu, L. J., Shen, S. Z., and Summons, R. E. (2008). Two episodes of ^{13}C-depletion in organic carbon in the latest Permian: evidence from the terrestrial sequences in northern Xinjiang, China. *Earth Planet. Sci. Lett.* 270, 251–257. doi:10.1016/j.epsl.2008.03.043

Chrzazvez, J., Théry-Parisot, I., Fiorucci, G., Terral, J.-P., and Thibaut, B. (2014). Impact of post-depositional processes on charcoal fragmentation and archaeobotanical implications: experimental approach combining charcoal analysis and biomechanics. *J. Archaeol. Sci.* 44, 30–42. doi:10.1016/j.jas.2014.01.006

Chu, D. L., Grasby, S. E., Song, H. J., Dal Corso, J., Wang, Y., Mather, T. A., et al. (2020). Ecological disturbance in tropical peatlands prior tomarine Permian-Triassic mass extinction. *Geology* 48, 288–292. doi:10.1130/g46631.1

Chu, D. L., Yu, J. X., Tong, J. N., Benton, M. J., Song, H. J., Huang, Y. F., et al. (2016). Biostratigraphic correlation and mass extinction during the Permian-Triassic transition in terrestrial-marine siliciclastic settings of South China. *Glob. Planet. Chang.* 146, 67–88. doi:10.1016/j.gloplacha.2016.09.009

Clark, J. S., and Patterson III, W. A. (1997). "Background and local charcoal in sediments: scales of fire evidence in the palaeo record," in *Sediment records of biomass burning and global change*. Editor J. S. Clark, H. Cachier, J. G. Goldammer, and B. Stocks, NATOASI Series I (Berlin: Springer Verlag), 23–48. doi:10.1007/978-3-642-59171-6_3

Cui, Y., Bercovici, A., Yu, J., Kump, L. R., Freeman, K. H., Su, S., et al. (2017). Carbon cycle perturbation expressed in terrestrial Permian–Triassic boundary sections in South China. *Global Planet. Change.* 148, 272–285. doi:10.1016/j.gloplacha.2015.10.018

Cui, Y., and Kump, L. R. (2015). Global warming and the end-Permian extinction event: proxy and modeling perspectives. *Earth Sci. Rev.* 149, 5–22. doi:10.1016/j.earscirev.2014.04.007

Dal Corso, J., Mills, B. J. W., Chu, D., Newton, R. J., Mather, T. A., Shu, W., et al. (2020). Permo-Triassic boundary carbon and mercury cycling linked to terrestrial ecosystem collapse. *Nat. Commun.* 11, 2962. doi:10.1038/s41467-020-16725-4

Diefendorf, A. F., Mueller, K. E., Wing, S. L., Koch, P. L., and Freeman, K. H. (2010). Global patterns in leaf ^{13}C discrimination and implications for studies of past and future climate. *Proc. Natl. Acad. Sci. USA* 107, 5738–5743. doi:10.1073/pnas.0910513107

El Atfy, H., Havlik, P., Krüger, P. S., Manfroi, J., Jasper, A., and Uhl, D. (2019). Pre-quaternary wood decay 'caught in the act' by fire – examples of plant–microbe interactions preserved in charcoal from clastic sediments. *Historical Biol.* 31, 952–961. doi:10.1080/08912963.2017.1413101

Erwin, D. H. (1994). The Permo-Triassic extinction. *Nature* 367, 231–236. doi:10.1038/367231a0

Fang, Q., Hong, H. L., Chen, Z. Q., Yu, J. X., Wang, C. W., Yin, K., et al. (2017). Microbial proliferation coinciding with volcanism during the Permian–Triassic transition: new, direct evidence from volcanic ashes, South China. *Palaeogeogr. Palaeoclimatol. Palaeoecol.* 474, 164–186. doi:10.1016/j.palaeo.2016.06.026

Favilli, F., Cherubini, P., Collenberg, M., Egli, M., Sartori, G., Schoch, W., et al. (2010). Charcoal fragments of Alpine soils as an indicator of landscape evolution during the Holocene in Val di Sole (Trentino, Italy). *Holocene* 20, 67–79. doi:10.1177/0959683609348850

Feng, Z., Wei, H. B., Guo, Y., He, X. Y., Sui, Q., Zhou, Y., et al. (2020b). From rainforest to herbland: new insights into land plant responses to the end-Permian mass extinction. *Earth Sci. Rev.* 204, 103153. doi:10.1016/j.earscirev.2020.103153

Feng, Z., Wei, H. B., Ye, R. H., Sui, Q., Gou, X. D., Guo, Y., et al. (2020a). Latest Permian peltasperm plant from Southwest China and its palaeoenvironmental implications. *Front. Earth Sci.* 8, 559430. doi:10.3389/feart.2020.559430

Glasspool, I. J. (2000). A major fire event recorded in the mesofossils and petrology of the Late Permian, Lower Whybrow coal seam, Sydney Basin, Australia. *Palaeogeogr. Palaeoclimatol. Palaeoecol.* 164, 357–380. doi:10.1016/S0031-0182(00)00194-2

Glasspool, I. J., and Scott, A. C. (2010). Phanerozoic atmospheric oxygen concentrations reconstructed from sedimentary charcoal. *Nat. Geosci.* 3, 627–630. doi:10.1038/ngeo923

Grasby, S. E., Sanei, H., and Beauchamp, B. (2011). Catastrophic dispersion of coal fly ash into oceans during the latest Permian extinction. *Nat. Geosci.* 4, 104–107. doi:10.1038/ngeo1069

Hall, G., Woodborne, S., and Scholes, M. (2008). Stable carbon isotope rations from archaeological charcoal as palaeoenvironmental indicators. *Chem. Geol.* 247, 384–400. doi:10.1016/j.chemgeo.2007.11.001

He, B., Xu, Y. G., Huang, X. L., Luo, Z. Y., Shi, Y. R., Yang, Q. J., et al. (2007). Age and duration of the Emeishan flood volcanism, SW China: geochemistry and SHRIMP zircon U-Pb dating of silicic ignimbrites, post-volcanic Xuanwei Formation and clay tuff at the Chaotian section. *Earth Planet. Sci. Lett.* 255, 306–323. doi:10.1016/j.epsl.2006.12.021

Heydari, E., Hassanzadeh, J., Wade, W. J., and Ghazi, A. M. (2003). Permian Triassic boundary interval in the Abadeh section of Iran with implications for mass extinction: Part 1-Sedimentology. *Palaeogeogr. Palaeoclimatol. Palaeoecol.* 193, 405–423. doi:10.1016/S0031-0182(03)00258-X

Hilton, J., Wang, S., Galtier, J., Glasspool, I., and Stevens, L. (2004). An Upper Permian permineralized plant assemblage in volcaniclastic tuff from the Xuanwei Formation, Guizhou Province, Southern China, and its paleofloristic significance. *Geol. Mag.* 141, 661–674. doi:10.1017/S0016756804009847

Hong, H. L., Algeo, T. J., Fang, Q., Zhao, L. L., Ji, K. P., Yin, K., et al. (2019). Facies dependence of the mineralogy and geochemistry of altered volcanic ash beds: an example from Permian-Triassic transition strata in southwestern China. *Earth Sci. Rev.* 190, 58–88. doi:10.1016/j.earscirev.2018.12.007

Jasper, A., Guerra-Sommer, M., Abu Hamad, A. M. A., Bamford, M., Bernardes-de-Oliveira, M. E. C., Tewari, R., et al. (2013). The burning of Gondwana: Permian fires on the southern continent—a palaeobotanical approach. *Gond. Res.* 24, 148–160. doi:10.1016/j.gr.2012.08.017

Jasper, A., Guerra-Sommer, M., Uhl, D., Bernardes-de-Oliveira, M. E., Ghosh, A. K., Tewari, R., et al. (2012). Palaeobotanical evidence of wildfires in the Upper Permian of India: macroscopic charcoal remains from the Raniganj formation, Damodar Valley Basin. *Palaeobotanist* 61, 75–82.

Jasper, A., Uhl, D., Agnihotri, D., Tewari, R., Pandita, S. K., Benício, J. R. W., et al. (2016a). Evidence of wildfires in the Late Permian (Changsinghian) Zewan formation of Kashmir, India. *Curr. Sci.* 110 (3), 419–423. doi:10.18520/cs/v110/i3/419-423

Jasper, A., Uhl, D., Tewari, R., Guerra-Sommer, M., Spiekermann, R., Manfroi, J., et al. (2016b). Indo-Brazilian Late Palaeozoic wildfires: an overview on macroscopic charcoal. *Geol. USP.* 16 (4), 87–97. doi:10.11606/issn.2316-9095.v16i4p87-97

Jin, Y. G., Wang, Y., Wang, W., Shang, Q. H., Cao, C. Q., and Erwin, D. H. (2000). Pattern of marine mass extinction near the Permian-Triassic boundary in South China. *Science* 289, 432–436. doi:10.1126/science.289.5478.432

Kauffmann, M., Jasper, A., Uhl, D., Meneghini, J., Osterkamp, I. C., Zvirtes, G., et al. (2016). Evidence for palaeo-wildfire in the Late Permian palaeotropics-charcoal from the Motuca formation in the Parnaíba Basin, Brazil. *Palaeogeogr. Palaeoclimatol. Palaeoecol.* 450, 122–128. doi:10.1016/j.palaeo.2016.03.005

Korte, C., Pande, P., Kalia, P., Kozur, H. W., Joachimski, M. M., and Oberhänsli, H. (2010). Massive volcanism at the Permian-Triassic boundary and its impact on the isotopic composition of the ocean and atmosphere. *J. Asian Earth Sci.* 37, 293–311. doi:10.1016/j.jseaes.2009.08.012

Krull, E. S., and Retallack, G. J. (2000). δ^{13}C depth profiles from paleosols across the Permian–Triassic boundary: evidence for methane release. *Bull. Geol. Soc. Am.* 112, 1459–1472. doi:10.1130/0016-7606(2000)112<1459:CDPFPA>2.0.CO;2

Krull, E. S., Lehrmann, D. J., Druke, D., Kessel, B., Yu, Y., and Li, R. (2004). Stable carbon isotope stratigraphy across the Permian-Triassic boundary in shallow marine carbonate platforms, Nanpanjiang Basin, South China. *Palaeogeogr. Palaeoclimatol. Palaeoecol.* 204, 297–315. doi:10.1016/S0031-0182(03)00732-6

Lancelotti, C., Madella, M., Ajithprasad, P., and Petrie, C. A. (2010). Temperature, compression and fragmentation: an experimental analysis to assess the impact of taphonomic processes on charcoal preservation. *Archaeol. Anthropol. Sci.* 2, 307–320. doi:10.1007/s12520-010-0046-8

Liu, H. Y., Wei, H. B., Chen, J., Guo, Y., Zhou, Y., Gou, X. D., et al. (2020). A latitudinal gradient of plant–insect interactions during the late Permian in terrestrial ecosystems? New evidence from Southwest China. *Global Planet. Chang.* 192, 103248. doi:10.1016/j.gloplacha.2020.103248

Lu, J., Zhang, P. X., Yang, M. F., Shao, L. Y., and Hilton, J. (2020). Continental records of organic carbon isotopic composition ($\delta^{13}C_{org}$), weathering, paleoclimate and wildfire linked to the End-Permian mass extinction. *Chem. Geol.* 558, 119764. doi:10.1016/j.chemgeo.2020.119764

Mahesh, S., Murthy, S., Chakraborty, B., and Roy, M. D. (2015). Fossil charcoal as palaeofire indicators: taphonomy and morphology of charcoal remains in sub-surface Gondwana sediments of South Karanpura Coalfield. *J. Geol. Soc. India.* 85, 1–10. doi:10.1007/s12594-015-0251-2

Manfroi, J., Uhl, D., Guerra-Sommer, M., Francischini, H., Martinelli, A. G., Soares, M. B., et al. (2015). Extending the database of Permian palaeo-wildfire on Gondwana: charcoal remains from the Rio do Rasto formation (Paraná Basin), Middle Permian, Rio Grande do Sul State, Brazil. *Palaeogeogr. Palaeoclimatol. Palaeoecol.* 436, 77–84. doi:10.1016/j.palaeo.2015.07.003

McParland, L. C., Collinson, M. E., Scott, A. C., and Campbell, G. (2009). The use of reflectance values for the interpretation of natural and anthropogenic charcoal assemblages. *Archaeol. Anthropol. Sci.* 1, 249–261. doi:10.1007/s12520-009-0018-z

Murthy, S., Mendhe, V. A., Kavali, P. S., and Singh, V. P. (2020). Evidence of recurrent wildfire from the Permian coal deposits of India: petrographic, scanning electron microscopic and palynological analyses of fossil charcoal. *Palaeoworld* 29, 1–14. doi:10.1016/j.palwor.2020.03.004

Nichols, G. J., Cripps, J. A., Collinson, M. E., and Scott, A. C. (2000). Experiments in waterlogging and sedimentology of charcoal: results and implications. *Palaeogeogr. Palaeoclimatol. Palaeoecol.* 164, 43–56. doi:10.1016/S0031-0182(00)00174-7

Peng, Y. Q., Yu, J. X., Gao, Y. Q., and Yang, F. Q. (2006). Palynological assemblages of non-marine rocks at the Permian–Triassic boundary, western Guizhou and eastern Yunnan, South China. *J. Asian Earth Sci.* 28, 291–305. doi:10.1016/j.jseaes.2005.10.007

Peters, M. E., and Higuera, P. E. (2007). Quantifying the source area of macroscopic charcoal with a particle dispersal model. *Quat. Res.* 67, 304–310. doi:10.1016/j.yqres.2006.10.004

Poole, I., Braadbaart, F., Boon, J. J., and van Bergen, P. F. (2002). Stable carbon isotope changes during artificial charring of propagules. *Org. Geochem.* 33, 1675–1681. doi:10.1016/S0146-6380(02)00173-0

Poole, I., Van Bergen, P. F., Kool, J., Schouten, S., and Cantrill, D. J. (2004). Molecular isotopic heterogeneity of fossil organic matter: implications for $\delta^{13}C$ biomass and $\delta^{13}C$ palaeoatmosphere proxies. *Org. Geochem.* 35, 1261–1274. doi:10.1016/j.orggeochem.2004.05.014

Retallack, G. J., and Jahren, A. H. (2008). Methane release from igneous intrusion of coal during Late Permian extinction events. *J. Geol.* 116, 1–20. doi:10.1086/524120

Scholze, F., Shen, S. Z., Backer, M., Wei, H. B., Hübner, M., Cui, Y. Y., et al. (2020). Reinvestigation of conchostracans (Crustacea: Branchiopoda) from late Permian–early Triassic sections in South China. *Palaeoworld.* 29, 368–390. doi:10.1016/j.palwor.2019.04.007

Schubert, B. A., and Jahren, A. H. (2012). The effect of atmospheric CO_2 concentration on carbon isotope fractionation in C_3 land plants. *Geochim. Cosmochim. Acta* 96, 29–43. doi:10.1016/j.gca.2012.08.003

Scott, A. C. (2010). Charcoal recognition, taphonomy and uses in palaeoenvironmental analysis. *Palaeogeogr. Palaeoclimatol. Palaeoecol.* 291, 11–39. doi:10.1016/j.palaeo.2009.12.012

Scott, A. C., and Glasspool, I. J. (2007). Observations and experiments on the origin and formation of inertinite group macerals. *Int. J. Coal Geol.* 70, 53–66. doi:10.1016/j.coal.2006.02.009

Scott, A. C. (1989). Observations on the nature and origin of fusain. *Int. J. Coal Geol.* 12, 443–475. doi:10.1016/0166-5162(89)90061-X

Scott, A. C. (2000). The pre-quaternary history of fire. *Palaeogeogr. Palaeoclimatol. Palaeoecol.* 164, 281–329. doi:10.1016/S0031-0182(00)00192-9

Shen, G. L. (1995). "Permian floras," in *Fossil floras of China through the geological ages*. Editor X. X. Li (Guangzhou: Guangdong Science and Technology Press), 127–208.

Shzen, S. Z., Crowley, J. L., Wang, Y., Bowring, S. A., Erwin, D. H., Sadler, P. M., et al. (2011). Calibrating the end-Permian mass extinction. *Science* 334, 1367–1372. doi:10.1126/science.1213454

Shen, S. Z., Cao, C. Q., Zhang, H., Bowring, S. A., Henderson, C. M., Payne, J. L., et al. (2013). High-resolution $\delta^{13}C_{carb}$ chemostratigraphy from latest Guadalupian through earliest Triassic in South China and Iran Earth. *Planet. Sci. Lett.* 375, 156–165. doi:10.1016/j.epsl.2013.05.020

Sugihara, N. G., Van Wagtendonk, J. W., and Fites-Kaufman, J. (2006). "Fire as an ecological process," in *Fire in California's ecosystems*. Berkeley: University of California Press, 58–74.

Svensen, H., Planke, S., Polozov, A., Schmidbauer, N., Corfu, F., Podladchikov, Y., et al. (2009). Siberian gas venting and the end-Permian environmental crisis. *Earth Planet. Sci. Lett.* 277, 490–500. doi:10.1016/j.epsl.2008.11.015

Tewari, R., Chatterjee, S., Agnihotri, D., and Pandita, S. K. (2015). Glossopteris flora in the Permian Weller formation of Allan Hills, South Victoria Land, Antarctica: implications for paleogeography, paleoclimatology, and biostratigraphic correlation. *Gond. Res.* 28, 905–932. doi:10.1016/j.gr.2015.02.003

Tieszen, L. L., and Boutton, T. W. (1989). "Stable carbon isotopes in terrestrial ecosystem research." in *Stable isotopes in ecological research*. New York, NY: Springer-Verlag, 68, 167–195.

Turekian, V. C., Macko, S., Ballentine, D., Swap, R. J., and Garstang, M. (1998). Causes of bulk carbon and nitrogen isotopic fractionations in the products of vegetation burns: laboratory studies. *Chem. Geol.* 152, 181–192. doi:10.1016/S0009-2541(98)00105-3

Turney, C. S. M., Wheeler, D., and Chivas, A. R. (2006). Carbon isotope fractionation in wood during carbonization. *Geochim. Cosmochim. Acta* 70, 960–964. doi:10.1016/j.gca.2005.10.031

Uhl, D., Butzmann, R., Fischer, T. C., Meller, B., and Kustatscher, E. (2012). Wildfires in the Late Palaeozoic and Mesozoic of the Southern Alps-the late Permian of the Bletterbach–Butterloch area (Northern Italy). *Riv. Ital. Paleontol. Stratigr.* 118, 223–233. doi:10.13130/2039-4942/6002

Uhl, D., Jasper, A., Abu Hamad, A. M. B., and Montenari, M. (2008). "Permian and Triassic wildfires and atmospheric oxygen levels. *Proc. WSEAS Conf. Spec. Iss.* 13, 179–187.

Uhl, D., and Kerp, H. (2003). Wildfires in the late palaeozoic of central Europe–the Zechstein (Upper Permian) of NW-Hesse (Germany). *Palaeogeogr. Palaeoclimatol. Palaeoecol.* 199, 1–15. doi:10.1016/S0031-0182(03)00482-6

Vajda, V., McLoughlin, S., Mays, C., Frank, T. D., Fielding, C. R., Tevyaw, A., et al. (2020). End-Permian (252 Mya) deforestation, wildfires and flooding—an ancient biotic crisis with lessons for the present. *Earth Planet. Sci. Lett.* 529, 115875. doi:10.1016/j.epsl.2019.115875

Wan, M. L., Zhou, W. M., Yang, W., and Wang, J. (2016). Charred wood of *prototaxoxylon* from the Wuchiapingian Wutonggou formation (Permian) of Dalongkou, Northern Bogda Mountains, Northwestern China. *Palaeoworld* 25 (1), 21–31. doi:10.1016/j.palwor.2015.06.003

Wang, G. A., Han, J. M., and Liu, D. S. (2003). Research of carbon isotope composition of C-3 herbaceous plant in loess region, North China. *Sci. China Ser. D* 6, 550–556 [in Chinese, with English summary]. doi:10.1360/02yd0384

Wang, H. (2011). *Sedimentological characteristics and palaeoenvironmental bearings of the Late Permian coals in eastern Yunnan and western Guizhou of southwestern China*. Beijing, China: China University of Mining and technology, 1–131.

Wang, J. (2015). *The Geochemistry of the coals at P/T boundary in Xuanwei, Yunnan and its paleoenvironmental significance*. Beijing,China: China University of Mining and technology, 1–167.

Wang, J. D., and Li, H. M. (1998). Paleo-latitude variation of Guizhou terrain from Devonian to cretaceous. *Chin. J. Geochem.* 17, 356–361. doi:10.1007/BF02837987

Wang, S. Y., and Yin, H. F. (2001). *Study on terrestrial permian-triassic boundary in Eastern Yunnan and Western Guizhou*. Wuhan: Press of China University of Geosciences, 88.

Wang, X. D., Cawood, P. A., Zhao, L. S., Chen, Z. Q., Lyu, Z. Y., and Ma, B. (2019). Convergent continental margin volcanic source for ash beds at the Permian Triassic boundary, South China: constraints from trace elements and Hf-isotopes. *Palaeogeogr. Palaeoclimatol. Palaeoecol.* 519, 154–165. doi:10.1016/j.palaeo.2018.02.011

Wang, Z. Q. (1993). On the occurrence of a plant-detritus taphocoenose from Permian-Triassic redbeds in Pingliang, Gansu. *Palaeoworld* 2, 152–162.

Wang, Z. Q., and Chen, A. S. (2001). Traces of arborescent lycopsids and dieback of the forest vegetation in relation to the terminal Permian mass extinction in North China. *Rev. Palaeobot. Palynol.* 117, 217–243. doi:10.1016/S0034-6667(01)00094-X

Wolbach, W. S., Lewis, R. S., and Anders, E. (1985). Cretaceous extinctions: evidence for wildfires and search for meteoritic material. *Science* 230, 167–170. doi:10.1126/science.230.4722.167

Xie, S. C., Pancost, R. D., Huang, J. H., Wignall, P. B., Yu, J. X., Tang, X. Y., et al. (2007). Changes in the global carbon cycle occurred as two episodes during the Permian–Triassic crisis. *Geology* 35, 1083–1086. doi:10.1130/G24224A.1

Xu, G., Feng, Q., Deconinck, J. F., Shen, J., Zhao, T., and Young, A. L. (2017). High-resolution clay mineral and major elemental characterization of a Permian-Triassic terrestrial succession in southwestern China: diagenetic and paleoclimatic/paleoenvironmental significance. *Palaeogeogr. Palaeoclimatol. Palaeoecol.* 481, 77–93. doi:10.1016/j.palaeo.2017.05.027

Yan, M. X., Wan, M. L., He, X. Z., Hou, X. D., and Wang, J. (2016). First report of Cisuralian (early Permian) charcoal layers within a coal bed from Baode, North China with reference to global wildfire distribution. *Palaeogeogr. Palaeoclimatol. Palaeoecol.* 459, 394–408. doi:10.1016/j.palaeo.2016.07.031

Yan, Z. M., Shao, L. Y., Glasspool, I. J., Wang, J., Wang, X. T., and Wang, H. (2019). Frequent and intense fires in the final coals of the Paleozoic indicate elevated atmospheric oxygen levels at the onset of the End-Permian mass extinction event. *Int. J. Coal Geol.* 207, 75–83. doi:10.1016/j.coal.2019.03.016

Yao, Z. Q., Xu, J. T., Zheng, Z. G., Zhao, X. H., and Mo, Z. G. (1980). "Late Permian biostratigraphy and problem of Permian–Triassic boundary in western Guizhou and eastern Yunnan," in *stratigraphy and palaeontology of Upper Permian coal-bearing formation in Western Guizhou and Eastern Yunnan*. Beijing, China: Science Press, 1–69.

Yu, J. X., Broutin, J., Chen, Z. Q., Shi, X., Li, H., Chu, D. L., et al. (2015). Vegetation changeover across the Permian-Triassic boundary in Southwest China: extinction, survival, recovery and palaeoclimate: a critical review. *Earth Sci. Rev.* 149, 203–224. doi:10.1016/j.earscirev.2015.04.005

Zhang, H., Cao, C. Q., Liu, X. L., Mu, L., Zheng, Q. F., Liu, F., et al. (2016). The terrestrial end-Permian mass extinction in South China. *Palaeogeogr. Palaeoclimatol. Palaeoecol.* 448, 108–124. doi:10.1016/j.palaeo.2015.07.002

Zhao, X. H., Mo, Z. G., Zhang, S. Z., and Yao, Z. Q. (1980). "Late Permian flora in Western Guizhou and Eastern Yunnan," in *Stratigraphy and palaeontology of upper Permian coal-bearing formation in Western Guizhou and Eastern Yunnan*. Beijing, China: Science Press, 1–69.

Zhong, Y. J., Huang, K. K., Lan, Y. F., and Chen, A. Q. (2018). Simulation of carbon isotope excursion events at the Permian-Triassic boundary based on GEOCARB. *Open Geosci.* 10 (1), 441–451. doi:10.1515/geo-2018-0034

Zhou, Y., Qin, H., and Zhang, C. B. (2014). Sedimentary environment and its evolution of the early Triassic Feixianguan formation in Huize, Yunnan Province. *Yunnan Geol.* 33, 172–179 [in Chinese, with English summary].

Conflict of Interest: The authors declare that the research was conducted in the absence of any commercial or financial relationships that could be construed as a potential conflict of interest.